Simple Quasispecies Models for the Survival-of-the-Flattest Effect: The Role of Space

Josep Sardanyés
Santiago F. Elena
Ricard V. Solé

SANTA FE INSTITUTE

Simple quasispecies models for the Survival-of-the-flattest effect: the role of space

Josep Sardanyés,[1] Santiago F. Elena,[2] and Ricard V. Solé[1, 3, *]

[1]*Complex Systems Lab (ICREA-UPF), Barcelona Biomedical Research Park (PRBB-GRIB)*
Dr. Aiguader 88, 08003 Barcelona, Spain
[2]*Instituto de Biología Molecular y Celular de Plantas, CSIC-UPV, 46022. València, Spain*
[3]*Santa Fe Institute, 1399 Hyde Park Road, Santa Fe NM 87501, USA*

The *survival-of-the-flattest* effect postulates that under high mutation rates natural selection does not necessarily favor the faster replicators. Under such conditions, genotypes which are robust against deleterious mutational effects may be favored instead, even at the cost of a slower replication. This tantalizing hypothesis has been recently proved using digital organisms, subviral RNA plant pathogens (viroids), and an animal RNA virus. In this work we study a simple theoretical system composed by two competing quasispecies which are located at two widely different fitness landscapes that represent, respectively, a fit and a flat quasispecies. The fit quasispecies is characterized by high replication rate and low mutational robustness whereas the flat quasispecies is characterized by low replication rate but high mutational robustness. By using a mean field model, *in silico* simulations with digital replicons and a two-dimensional spatial model given by a stochastic cellular automata (CA), we predict the presence of an absorbing first-order phase transition with *critical slowing down* between selection for replication speed and selection for mutational robustness, where the surpassing of a critical mutation rate involves the outcompetition of the fit quasispecies by the flat one. Furthermore, it is shown that space, which involves a lower critical mutation rate, broadens the conditions at which the *survival-of-the-flattest* may occur.

Keywords: survival-of-the-flattest, quasispecies spatial dynamics, robustness, virus evolution, critical phenomena, absorbing first-order phase transitions.

I. INTRODUCTION

The quasispecies theory of molecular evolution, originally developed by M. Eigen and collaborators (Eigen et al. 1988, Eigen and Schuster 1979) has become the standard theoretical framework used to model the evolution of RNA viruses (Domingo 2002, Domingo and Holland 1997). One of the keystones of theoretical quasispecies, shared by RNA viruses, is that replication fidelity is so low that the number of mutant offspring generated in a population may exceed the number of offspring identical to the parental genotype. This gives rise to highly polymorphic populations in which the frequency of the wildtype and of each mutant genotype not only depends on their replication rates but also on their constant genesis by mutation from genotypes which are close in genotypic space. In a constant environment and in the absence of other external perturbations, this distribution of genotypes is known as the quasispecies (Eigen et al. 1988).

The existence of a population structure in quasispecies strongly affects the way selection acts, because the evolutionary success of individual genomes does not depend anymore on their own replication rate but also on the average growth rate of the quasispecies they belong to. Fast replicating genomes that produce low-fitness offspring can be outcompeted by slow replicating genomes provided the latter inhabits a region of sequence space characterized by high neutrality and connectivity (Schuster and Swetina 1988, van Nimwegen et al. 1999, Wilke 2001b). This phenomenon has been dubbed as the *quasispecies effect* (van Nimwegen et al. 1999,

Wilke 2001a) or more recently as the *survival-of-the-flattest* (Wilke et al. 2001) in clear reference to Darwin's *survival-of-the-fittest* concept. Indeed, authors who have casted doubts about the relevance of the quasispecies model to real viruses based their criticism in the fact that the quasispecies effect was never observed *in vivo* (Holmes and Moya 2002, Jenkins et al. 2001). However, two recent experiments give strong support to the validity of the quasispecies effect for real viral populations. In the first experiment, two viroids (small circular RNAs that infect plants and do not encode for any protein) populations were allowed to compete at increasing mutation rates (Codoñer et al. 2006). At low mutation rate the faster but genetically homogeneous replicator outcompeted the slower but highly polymorphic one, as expected from the survival-of-the-fittest effect. However, the result of the competition was reversed at high mutation rate and the slower replicator won the competition by taking advantage of its larger mutational robustness. In the second study (Sanjuán et al. 2007), two populations of *Vesicular stomatitis virus* (VSV) that differed in their replication rates and robustness competed at increasing concentrations of chemical mutagens. Below a certain concentration of mutagens, the fittest VSV outcompeted the flattest one. Above this critical concentration, the competition result was reverted and the flattest VSV systematically displaced the fittest one.

One peculiarity of viral infections that is usually ignored by most quasispecies models is the existence of a spatial population structure. Only a few studies have analyzed the error-threshold transition in a spatial context (Altemeyer and McCaskill 2001, Toyabe and Sano 2005). It is well known that spatial dynamics can deeply change the outcome of competition even under the absence of selection (Solé and Bascompte 2006). Within infected hosts, viruses do not behave as a single well-stirred population but as a collection of subpopulations

_____

[*] Author for correspondence: e-mail: ricard.sole@upf.edu;
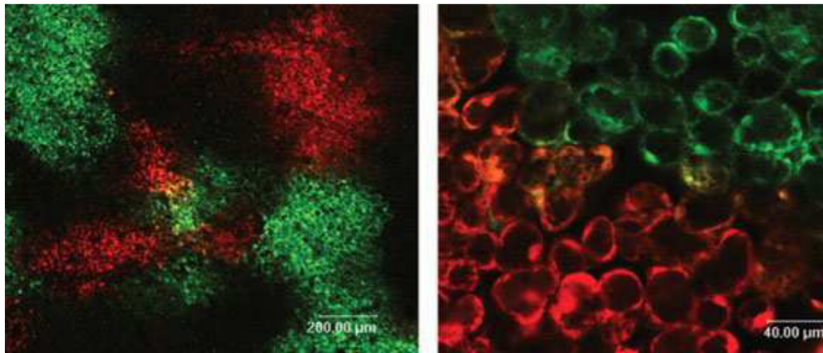Phone: +34 933160532; Fax: +34 933160550

FIG. 1: Spatial distribution of two PPV variants infecting the same leaf of *N. benthamiana*. Each variant was labeled with a different fluorescent protein (red and green). Coinfected shall appear as yellow fluorescent. The right panel is a 5-fold magnification of the left one, and shows that only the line of cells at the confluence edge can be infected by the two PPV variants (taken from Dietrich and Maiss (2003)).

that colonize and reproduce on different compartments constituted by different tissues and organs. For example, it has been extensively shown that after infection, the *Human immunodeficiency virus* type 1 (HIV-1) is able to establish well-differentiated populations which are organ-specific and show limited gene flow among them (Bordería et al. 2007, Sanjuán et al. 2004). In these cases, organ-specificity appears not as a consequence of founder events but as a consequence of differences in the adaptive constraints imposed by heterogeneous cell types and the existence of fitness tradeoffs across organs. In the case of plant viruses, spatial structure appears at two different levels. First, it has been shown that different leaves can be infected with different viral subpopulations, which, for the case of perennial plants, may further differentiate into different branches and sub-branches, as it has been shown, for example, for *Plum pox virus* (PPV) (Jridi et al. 2006). In this case, population structure likely arises as a consequence of the strong bottlenecks associated with the systemic movement of viruses from source to sink leaves (Hall et al. 2001, Li and Roossinck 2004, Sacristán et al. 2003). Second, within a given infected leaf, that for the sake of simplicity can be considered as a two dimensional space, populations initiated at different infectious foci do not overlap after confluence but exclude each other, generating a patched distribution of genotypes (Dietrich and Maiss 2003) (see Fig. 1).

In the present report we analyze the dynamics of two competing quasispecies by using a simple mean field model, *in silico* simulations with digital replicons, and a stochastic cellular automata (CA) model, which allows to simulate the competition process explicitly considering the potential effect of physical space. In all these approaches, the fit quasispecies has a fast replication rate but is surrounded by genotypes which are strongly deleterious and thus mutations always have a strong negative effect on the average population fitness. On the contrary, the flat one has a lower replication rate but is located at a neutral and highly connected region of sequence space, and thus mutations exert a mild impact on viral fitness. In particular, we are interested in studying the effect of increasing mutation rate on the outcome of the competition process, paying special attention to the role of spatial structure. In short,

our results suggest the existence of a critical mutation rate at which an absorbing first-order phase transition with slowing down between selection for fast replication and selection for mutational robustness takes place. Beyond the critical mutation rate, the flat quasispecies outcompetes the fit one. In the vicinity of this transition both quasispecies can coexist during an extremely long time. Moreover, space is shown to broaden the conditions at which the survival-of-the-flattest can be observed. The results of the *in silico* simulations are in complete agreement with the mean field analysis.

II. QUASISPECIES MEAN FIELD MODEL

As a first approach to the analysis of the competition dynamics between two quasispecies located at two different fitness landscapes, a mean field model has been used. The model considers a perfectly mixed system with a fit quasispecies, x, and a flat one, y. Under the assumption $\sum_i (x_i + y_i) = 1$, the model is defined by the following set of ODEs:

$$\frac{dx_0}{dt} = f_x^{(0)} Q x_0 - x_0 \Phi(\mathbf{x}, \mathbf{y}) - \epsilon x_0, \tag{1}$$

$$\frac{dx_1}{dt} = f_x^{(0)}(1-Q)x_0 + f_x^{(1)}x_1 - x_1 \Phi(\mathbf{x}, \mathbf{y}) - \epsilon x_1, \tag{2}$$

$$\frac{dy_0}{dt} = f_y^{(0)} Q y_0 + f_y^{(1)} y_1 (1-Q) - y_0 \Phi(\mathbf{x}, \mathbf{y}) - \epsilon y_0, \tag{3}$$

$$\frac{dy_1}{dt} = f_y^{(1)} Q y_1 + f_y^{(0)} y_0 (1-Q) - y_1 \Phi(\mathbf{x}, \mathbf{y}) - \epsilon y_1, \tag{4}$$

where the term $\Phi(\mathbf{x}, \mathbf{y}) = \sum_{i=0,1}[(f_x^{(i)} - \epsilon)x_i + (f_y^{(i)} - \epsilon)y_i]$, indicates the outflow (i.e., excess production) defining a constant population (CP) constraint. Here x_0 denotes the relative concentration of the master sequence and x_1 the concentration of all the mutant sequences, which are grouped in an average sequence different form the master one. The self-replication
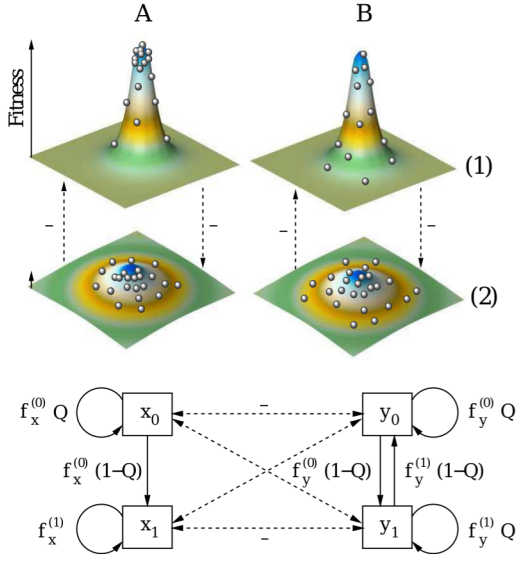
FIG. 2: The fit (1) and the flat (2) quasispecies are located at two different fitness landscapes. At low mutation rate (A) populations are centered on the peak; at high mutation rate (B) populations drift on the landscape away from the peak. The lower diagram provides a schematic representation of the quasispecies competition model (section II). Dashed arrows indicate the competition among both quasispecies.
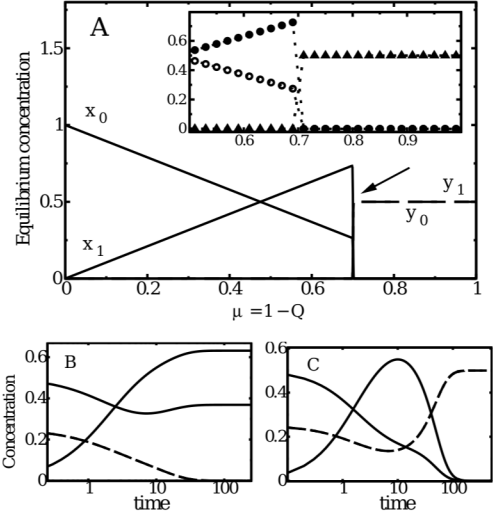

FIG. 3: (A) Equilibrium concentrations at increasing mutation rate with $f_x^{(0)} = 1$, $f_x^{(1)} = 0.05$, $f_y^{(0)} = f_y^{(1)} = 0.3$, and $\epsilon = 0$. The inset shows an enlarged view of the sharp transition point indicated with the arrow. Here x_0, x_1, y_0 and y_1 are represented as open circles, closed circles, filled and open triangles, respectively. Here the initial conditions were: $x_0(0) = 0.35$, $x_1(0) = 0.2$, $y_0(0) = 0.15$, $y_1(0) = 0.3$. The time dynamics associated to the survival-of-the-fittest and to the-survival-of-the-flattest are shown in (B) and (C) (x_0: thick solid line; x_1: thin solid line; y_0: thick dashed line; and y_1: thin dashed line), with same parameter values as in (A) with $Q = 0.4$ (B), and $Q = 0.25$ (C). Here, for both scenarios, we use: $x_0(0) = 0.5$, $x_1(0) = 0$, $y_0(0) = y_1(0) = 0.25$.

rate for the master sequence is given by $f_x^{(0)}$, while the self-replication constant for the other sequences (grouped in x_1) is $f_x^{(1)}$. Here, as a consequence of the assumed fitness landscape, the master sequence x_0 replicates faster than the pool of mutants x_1 and thus $f_x^{(0)} \gg f_x^{(1)}$. Both variables y_0 and y_1 indicate the relative concentration of the flat quasispecies, which is a densely connected one because is located in a flat fitness landscape and thus backward mutations are allowed to happen (see Fig. 2). Finally, ϵ denotes the decay rate for the replicators, which is defined to be the same for both quasispecies. Note that our model allows us to study two different scenarios considering both no decay ($\epsilon = 0$) and decay ($\epsilon \neq 0$).

Hereafter we will assume that $f_y^{(0)} = f_y^{(1)} = f_y < f_x^{(0)}$. In all the equations Q denotes the average quality factor of self-replication, which we assume to be the same for all the sequences, thus being the mutation rate, μ, defined as $\mu = 1 - Q$. The qualitative behavior of Eqs. (1-4) can be studied by means of linear stability analysis of the equilibrium points. Note that the concentration equilibrium for both flat quasispecies is the same i.e., $y_0^* = y_1^*$, because we have assumed that their self-replication rates are equal, thus becoming both Eqs. (3-4) symmetric. Hence, in order to simplify our model we can reduce the system (1-4) to a three-dimensional dynamical system by considering $\sum_i \dot{y}_i = \dot{y}$ and $y_0 + y_1 = y$, thus having $\dot{y} = f_y y - y \Phi(\mathbf{x}, y) - \epsilon y$. It can be shown that this reduced system has four fixed points, given by: $P^*(\mathbf{0})$, $P^*(0, 0, 1)$,

$P^*(0, 1, 0)$ and $P^*(x_0^*, 1 - x_0^*, 0)$, with:

$$x_0^* = \frac{f_x^{(0)}Q - f_x^{(1)}}{f_x^{(0)} - f_x^{(1)}}. \tag{5}$$

For the sake of simplicity, linear stability analysis is done by setting $\epsilon = 0$. It is easy to show that the fixed point $P^*(\mathbf{0})$ is always unstable when self-replication rates are higher than zero, since the eigenvalues obtained from the Jacobi matrix, $L(\mathbf{0})$, are $\lambda^{(1)} = f_x^{(0)}Q$, $\lambda^{(2)} = f_x^{(1)}$ and $\lambda^{(3)} = f_y$. Thus all these eigenvalues will be positive or zero (when self-replications rates are zero). Let us now analyze the most interesting case, that is, the survival-of-the-flattest scenario, corresponding to the fixed point $P^*(0, 0, 1)$. The stability of this point is obtained from the eigenvalues of $L(0, 0, 1)$, which are given by: $\lambda^{(1)} = f_x^{(0)}Q - f_y$, $\lambda^{(2)} = f_x^{(1)} - f_y$, and by $\lambda^{(3)} = -f_y$. Note that $\lambda^{(2,3)} < 0$, since it is assumed that $f_y > f_x^{(1)}$. From $\lambda^{(1)}$ we can derive the critical mutation rate which makes this fixed point becoming stable i.e., $\lambda^{(1)} < 0$, thus indicating that the flat quasispecies will be the surviving one. Such a critical condition is defined to be:

$$\mu_c = 1 - \frac{f_y}{f_x^{(0)}}. \tag{6}$$

Hence, the survival-of-the-flattest will take place provided $\mu > \mu_c$. The stability properties for the third fixed point
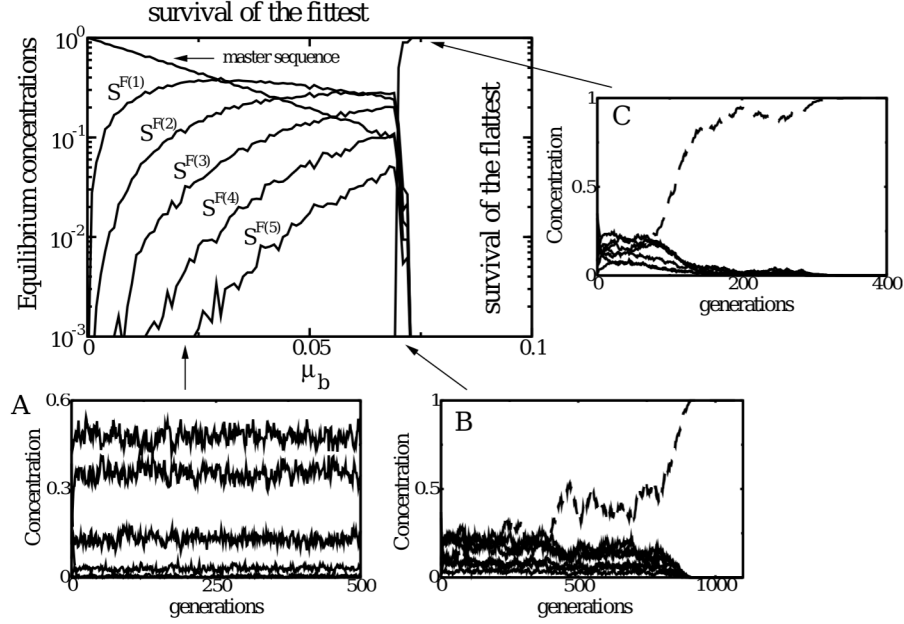
FIG. 4: Normalized equilibrium concentrations (in linear-log plot) as a function of per-bit mutation probability, μ_b, with $r_p = 10^{-3}$ and $r_f = 0.1$ (after discarding 5000 generations and averaging over 10 independent runs). The curves below the master sequence correspond (from top to bottom) to the mutant sequences of the fit quasispecies differing up to five bits from the master sequence. Note that beyond $\mu_b^c \approx 0.072$, the flat quasispecies (thick line) is able to outcompete the fit one. The arrows indicate the per-bit mutation probabilities used to display the time dynamics of both quasispeces: (A) survival-of-the-fittest-scenario with $\mu_b = 0.023$; (B) very near the critical mutation with $\mu_b = 0.07$; and (C) survival-of-the-flattest scenario with $\mu_b = 0.078$. In all the time plots: master sequence (solid thick line), mutants differing up to five bits from the master sequence (solid thin lines), and the normalized sum of the sequences belonging to the flat quasispecies (dashed thick line).

$P^*(0, 1, 0)$, are obtained from the eigenvalues of $L(0, 1, 0)$, which are given by $\lambda^{(1)} = f_x^{(0)}Q - f_x^{(1)}$, $\lambda^{(2)} = -f_x^{(1)}$, and by $\lambda^{(3)} = f_y - f_x^{(1)}$. Note that $\lambda^{(2)}$ is always negative, and $\lambda^{(3)}$ is always positive because $f_y > f_x^{(1)}$, being such a point a saddle (since $\lambda^{(3)}$ involves an unstable subspace). Moreover, $\lambda^{(1)}$ is positive when $Q > f_x^{(1)}/f_x^{(0)}$. As $f_x^{(0)} \gg f_x^{(1)}$, $\lambda^{(1)}$ will also be tipically positive. The stability of the last fixed point is analyzed from $L(x_0^*, 1 - x_0^*, 0)$. The eigenvalues for this case are: $\lambda^{(1)} = -f_x^{(0)}Q$, $\lambda^{(2)} = f_y - f_x^{(0)}Q$, and $\lambda^{(3)} = f_x^{(1)} - f_x^{(0)}Q$. Note that $\lambda^{(1)}$ is always negative. Hence, this point will be stable if $f_x^{(0)}Q > f_y$ and $f_x^{(0)}Q > f_x^{(1)}$.

The temporal dynamics of Eqs. (1-4) has also been numerically studied using the standard fourth-order *Runge-Kutta* method with a constant time step $\delta t = 0.1$ (assuming $f_x^{(0)} = 1 \gg f_x^{(1)} = 0.05$, $f_y^{(0)} = f_y^{(1)} = 0.3 < f_x^{(0)}$, and $\epsilon = 0$). Numerical results are in agreement with linear stability analysis. In Fig. 3A we compute the equilibrium concentration (after discarding the transient period) at increasing mutation rates. The inset clearly shows that such a concentration decreases for the fit quasispecies (x_0), and increases for the pool of mutants (x_1). Once the critical mutation is overcome, the fit quasispecies becomes extinct, and the flat one achieves a non-trivial stationary concentration. In the same figure we also show the time dynamics of the system below (Fig. 3B) and above (Fig.

3C) the critical mutation rate. Figure 3A indicates the presence of a sharp change in the qualitative dynamics once the critical mutation rate is overcome. Such a result can be interpreted as an absorbing first-order phase transition among the survival-of-the-fittest and the survival-of-the-flattest scenarios, in agreement with the study of Wilke (2001b). The extinction time of these quasispecies hyperbolically diverges in the vicinity of the critical mutation point, being extremely long very near the phase transition point (results not shown). This actually corresponds to a phenomenon of critical slowing down in the vicinity of the phase transition.

III.   *IN SILICO* BIT STRING MODEL

Next, we extended the previous mean field model by considering two competing populations of quasispecies in the form of binary digital replicators, thus considering the whole mutant spectrum of the quasispecies, within a multidimensional sequence space. This computational approach has been previously used to study viral dynamics and evolution (Codoñer et al. 2006, Solé et al. 1999; 2006). Let us define two populations of digital replicons, given by a fit quasispecies, $\mathbf{S}_i^F$, and a flat one, $\mathbf{S}_i^f$, both of them defined as populations composed of binary strings named $\mathbf{S}_i^{F,f} = (S_{i1}^{F,f}, ..., S_{i\nu}^{F,f})$, with $S_{ij}^{F,f} \in \{0, 1\}$, being ν the sequence length, where

$i = 1, ..., N$, being N the maximum population number of sequences (we use $\nu = 32$ and $N = 500$). The fit quasispecies is formed by the master sequence (all-ones string) and its entire mutant spectrum (all the other $2^\nu - 1$ sequences). The master sequence is assumed to self-replicate at the maximum probability (i.e. $r_m = 1$). The pool of mutants self-replicates with a lower probability, $r_p = 10^{-3}$, because we also assume that the fit quasispecies is located at a sharp fitness landscape and mutations have large deleterious effects. On the contrary, the flat quasispecies corresponds to a robust neutral network in which mutations do not affect self-replication rates. Thus all possible sequence combinations for the flat quasispecies self-replicate at $r_f = 0.1$.

As initial conditions we randomly inoculate the population with master sequences of the fit quasispecies and with random flat quasispecies. At each generation in the algorithm the following set of rules was repeated N times:

1. A string from the population was randomly chosen and replicated according to the above-mentioned probabilities.

2. Replication takes place by replacing one of the strings in the population (also taken at random) say $S_{j\neq i}$, by a copy of S_i. The self-replication mechanism presents error at rates μ_b, per bit and replication cycle, respectively.

Figure 4 shows the average equilibrium concentration as a function of the per-bit mutation probability for three different types of sequences: the master string; some sequences of the mutant spectrum of the fit quasispecies (i.e., the five nearest hypercubic orthant neighbors given by the sequences differing up to five bits from the master one); and the flat quasispecies (represented with the normalized sum of all the sequences belonging to this quasispecies) at increasing mutation probabilities. From this diagram, the critical mutation probability is shown to be $\mu_b \approx 0.072$. In order to compare this critical mutation rate with the one obtained with the mean field model we must take into account that μ_b is the per-bit mutation probability. The probability of error-free copy of the master sequence is given by $(1 - \mu_b)^\nu$, and thus the probability that at least one bit will be copied with error is:

$$\mu = 1 - (1 - \mu_b)^\nu. \qquad (7)$$

According to expression (7), the critical mutation rate obtained from $\mu_b^c = 0.072$, is $\mu_c = 0.908$. The value predicted with the mean field model (i.e., expression (6)), using the self-replication probabilities as replication rates, is given by $\mu_c = 0.9$. Note that this mutation value perfectly matches with the one analytically derived from the mean field model. Figure 4 also shows three examples of the time evolution of the sequences used in the diagram. Specifically, in Fig. 4A we display the scenario below the critical per-bit mutation, where the master sequence (solid thick line) achieves a higher stationary concentration than the mutant strings (from top to down we can follow the time evolution from the first to the
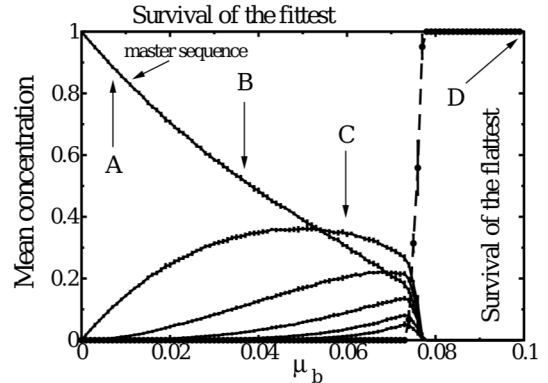

FIG. 5: Quasispecies populations at increasing per-bit mutation rates for the spatial model, with $L = 128$, $f_{pool} = 0.05$, $f_m = 1$, $f_{flat} = 0.1$ and $\epsilon = 0.01$ (each data point is the mean concentration $\pm$ standard deviations averaged over 5 replicas after discarding $\tau = 2 \times 10^5$ generations). The flat quasispecies (considering the whole population of strings) is indicated with the empty circles and the dashed line. Below the master sequence we show (from top to bottom) the strings differing up to five bits from the master sequence. The capital letters indicate the mutation probabilities used in Fig. 6.

fifth neighbor in sequence space). Figure 4B shows the time dynamics near the critical mutation. For this particular run, the flat quasispecies was able to outcompete the fit one. Note that the master sequence and the strings forming the pool of mutants become extinct at approximately 900 generations. If mutation probability is increased the same outcome is found although the fit quasispecies becomes extinct earlier (see Fig. 4C).

IV. BIT STRING SPATIAL MODEL

We finally develop a spatially-extended stochastic model including the whole quasispecies structure of both competing quasispecies. We define a $L \times L$ state space $\Omega(L) \in \mathbb{Z}^2$, with zero-flux boundary conditions (simulating, for example, the bounded system of plant leaves). Each quasispecies (the fit, $\mathbf{S}_i^F = (s_{i1}^F, ..., s_{i\nu}^F)$, and the flat, $\mathbf{S}_i^f = (s_{i1}^f, ..., s_{i\nu}^f)$) have a potential population composed of $|\mathcal{H}^\nu|$ (with $\mathcal{H} = 2$ and $\nu = 16$) binary strings which define the states of the automaton and correspond to the whole spectrum of strings living in the vertices of two 16-th dimensional Boolean hypercubes. We choose, at each generation τ, $L \times L$ random cells to ensure an average updating of all the lattice cells per generation. Assuming that only a single bit string can occupy a lattice cell and a Moore neighborhood for replication events, we apply two state transition rules (with same probability), according to:

1. **Self-replication**: If the cell is occupied by a sequence of the fit quasispecies, $\mathbf{S}_i^F$, and the neighbor site is empty, $\mathbf{S}_i^F$ replicates with probability $f_m \in [0, 1]$ if it is the master sequence, $\mathbf{S}_m^F$ (i.e., all-ones string), according to the next reactions:
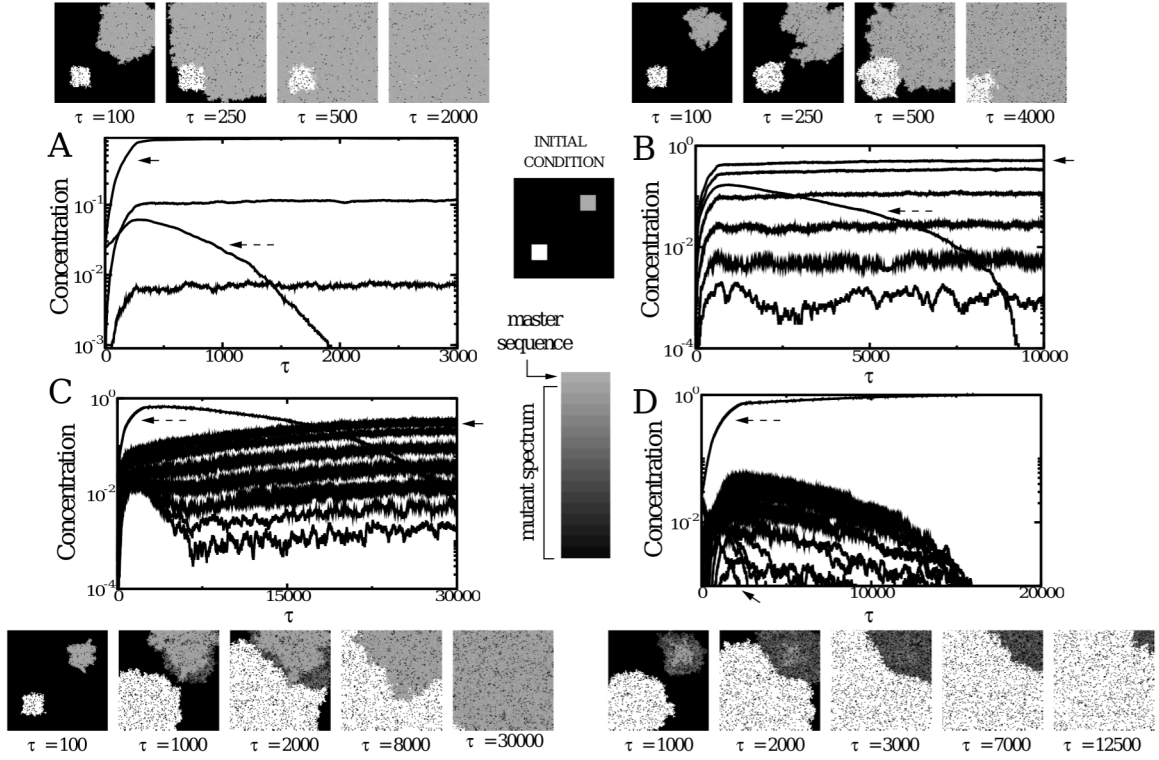
FIG. 6: Spatio-temporal dynamics for the CA model with same probabilities as in Fig. 5, and: (A) $\mu_b = 0.0075$; (B) $\mu_b = 0.0375$; (C) $\mu_b = 0.06$; and (D) $\mu_b = 0.1$. For time dynamics (in linear-log scale): flat quasispecies (dashed arrow), master sequence of the fit quasispecies (solid arrow), pool of deleterious mutants of the fit quasispecies (the other time trajectories). In the snapshots obtained from the time series we show: flattest strings (white); empty cells (black); fit quasispecies (gray gradient represented in the middle of the figure). Here the upper gray band corresponds to the master sequence and the rest of colors (from top to bottom) to the sequences differing from one to sixteen bits from the master sequence. As initial conditions (middle) we inoculated the lattice with two patches containing all-one sequences for both flat and fit quasispecies.

$$\mathbf{S}_m^F + \phi \xrightarrow{f_m(1-\mu)^\nu} 2\mathbf{S}_m^F,$$

$$\mathbf{S}_m^F + \phi \xrightarrow{f_m W_{ij}} \mathbf{S}_m^F + \mathbf{S}_{j\neq m}^F.$$

If the cell is occupied by a deleterious mutant of the fit quasispecies, it replicates to an empty neighbor site with probability $f_{pool} \in [0,1]$, according to the following pair of reactions:

$$\mathbf{S}_{i\neq m}^F + \phi \xrightarrow{f_{pool}(1-\mu)^\nu} 2\mathbf{S}_{i\neq m}^F,$$

$$\mathbf{S}_{i\neq m}^F + \phi \xrightarrow{f_{pool}W_{ij}} \mathbf{S}_{i\neq m}^F + \mathbf{S}_{j\neq i}^F.$$

If the cell is occupied by a string of the flat quasispecies, it replicates towards an empty neighbor with probability $f_{flat} \in [0,1]$, according to:

$$\mathbf{S}_i^f + \phi \xrightarrow{f_{flat}(1-\mu)^\nu} 2\mathbf{S}_i^f,$$

$$\mathbf{S}_i^f + \phi \xrightarrow{f_{flat}W_{ij}} \mathbf{S}_i^f + \mathbf{S}_{j\neq i}^f,$$

2. **Decay**: If the cell is occupied by a string, it decays with probability $\epsilon \in [0,1]$, leaving a free space according to:

$$\mathbf{S}_i \xrightarrow{\epsilon} \phi.$$

We use: $f_m = 1$, $f_{pool} = 0.05$, $f_{flat} = 0.1$ and $\epsilon = 0.01$. The terms W_{ij} correspond to the probabilities of erroneous replication and are given by $W_{ij} = (1-\mu)^{\nu-d_H[\mathbf{S}_i,\mathbf{S}_j]} \cdot \mu^{d_H[\mathbf{S}_i,\mathbf{S}_j]}$, being $d_H[\mathbf{S}_i,\mathbf{S}_j] = \sum_{k=1}^{\nu}|s_i^k - s_j^k|$, the Hamming distance between the two sequences. As initial conditions two patches were inoculated with all-one sequences for both populations (see Fig. 6 middle).

We investigate the effect of increasing mutation rate in the population structure of both competing quasispecies. The results show an approximate linear decay in the concentration
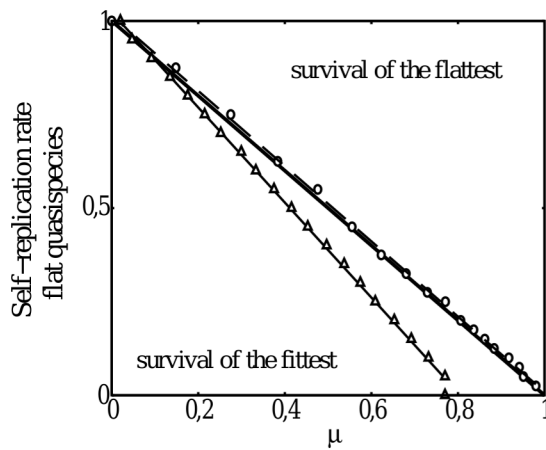
FIG. 7: Critical mutation rates as a function of self-replication rate of the flat quasispecies. We show the values of μ_c predicted by the mean field model (thick solid line) with $f_x^{(0)} = 1$ and $\epsilon = 0$. For the *in silico* model (white circles, with $r_m = 1$ and $r_p = 0.05$), we plot the value of the lower mutation probability involving (after 3000 generations) a whole population composed by flattest strings. For the CA model (triangles) we compute (using Eq. (7)) the lower mutation probability involving the outcompetition of the fit quasispecies by the flat one with $f_m = 1$, $f_{pool} = 0.05$, $\epsilon = 0.05$ and $L = 128$ (the same critical mutation values are found for $L = 40$, $L = 80$, and $L = 200$ (results not shown)). Dashed and thin solid lines correspond, respectively, to linear regressions for the critical mutation values for the bit string model of section III and for the CA model.

of the master sequence of the fit quasispecies as mutation rate increases. The flat quasispecies can outcompete the fit one beyond $\mu_b \approx 0.079$ (see Fig. 5). The spatiotemporal dynamics associated to four different mutation probabilities is shown in Fig. 6. The first one (Fig. 6A) shows the dynamics with low per-bit mutation rate ($\mu_b = 0.0075$). As mutation rate is low, the master sequence of the fit quasispecies (solid arrow) rapidly spreads, invading the space and outcompeting the flat replicator (dashed arrow). The time evolution for the mutant sequences differing in 1 (up) and in 2 (down) bits from the master sequence of the fit quasispecies are also shown. These are actually the only sequences found in the mutant spectrum since mutation is very low.

If mutation rate is increased up to $\mu_b = 0.0375$, the master sequence of the fit quasispecies grows slowly, and the mutant spectrum contains a higher diversity of sequences (see Fig. 6B). The mutant sequences belonging to the fit quasispecies (from top to down) differing in up to five bits from the master sequence are specifically shown. Actually, the sequences differing in more than 6 zeros from the master sequence are not found in the pool of mutants (results not shown). The third case (Fig. 6C) shows the dynamics with a mutation rate near to the critical value. Here, the fit quasispecies asymptotically outcompetes the flat one. Note that the diversity of sequences of the mutant spectrum increases (for this case we find sequences differing in 1 to 9 zeros from the master sequence). As we are near the transition point, the time that the fit quasispecies spends in outcompeting the flat one is longer,

in agreement with the previous models which showed the critical slowing down phenomenon. The dynamics with $\mu_b = 0.1$ are shown in Fig. 6D. Here the per-bit mutation value is above the critical mutation probability and thus the flat quasispecies outcompetes the fit one. Now all possible sequences of the mutant spectrum appear, and the master sequence of the fit quasispecies (small solid arrow) rapidly extincts (approximately after $\tau = 2200$ generations).

In Fig. 7 we represent the critical mutation value for all the models analyzed in this work. Interestingly, the values of μ_c obtained for the CA model, in which space is explicitly incorporated, are systematically below the values obtained for those models that do not consider spatial structure (i.e., mean field and bit-string models), strongly suggesting that replication on a spatially constrained scenario rather than in a well-stirred environment enlarges the parameter space at which the survival-of-the-flattest may occur. The $f_y(\mu_c)$ function is easily derived from the spatially mixed case, from Eq. (6):

$$f_y(\mu_c) = f_x^{(0)}(1 - \mu_c),$$

which will be maximal for $\mu_c = 0$ and zero at $\mu_c = 1$ (as expected). The spatial model also follows a linear relation, but it now decays as:

$$f_y^S(\mu_c) = f_x^{(0)}(1 - \alpha(\epsilon, \nu)\mu_c),$$

where $\alpha(\epsilon, \nu)$ is some (to be analyzed elsewhere) function of spatial constraints, decay and -presumably- genome length. This deviation between the spatial and non-spatial counterparts of the string model seems consistent with previous work by Altemeyer and McCaskill on error threshold for spatially extended quasispecies (Altemeyer and McCaskill 2001) (see also (Toyabe and Sano 2005)). In their study, this authors showed that decreased diffusion in a given spatial domain leads to a decrease in the error threshold mutation. Here a related phenomenon is being observed within the context of competing quasispecies.

V. DISCUSSION

In the present work we have explored the dynamics of competition between two quasispecies located at two widely different fitness landscapes that correspond, respectively, to a high-fitness and low-robustness (the fittest landscape) and to a low-fitness and high-robustness (the flattest landscape) scenarios. The effect of different mutation rates on the outcome of the competition between these two quasispecies has been explored. A mean field model, *in silico* simulations with binary digital replicators and a spatially-explicit model given by a stochastic two dimensional cellular automata (CA) have been employed. All these approaches show, in agreement with previous studies (Codoñer et al. 2006, Sanjuán et al. 2007, Wilke 2001a, Wilke et al. 2001), that under high mutation rates the flat quasispecies are advantaged, and thus selection positively acts on robustness more strongly than on replication speed.

The mean field analysis has allowed us to derive an analytical solution for the critical mutation rate, μ_c, at which an absorbing first-order phase transition with critical slowing down between selection for fast replication and selection for robustness takes place. In previous work, the numerical value of μ_c was obtained as the solution of a quadratic expression (Wilke et al. 2001) and, hence, it was not straightforward to visualize the effect that the different parameters involved in the expression (replication rate and robustness) had on μ_c. Our estimator of μ_c, however, has a much simpler expression since only depends on the ratio between the self-replication rates of the flat quasispecies, f_y, and the master sequence (i.e., the mutation-free genotypes), $f_x^{(0)}$, of the fit quasispecies. The larger the difference in replication rates between these two quasispecies, the smaller the value of μ_c and therefore, the easier to observe the survival-of-the-flattest effect.

We have also extended the analysis of these theoretical quasispecies performing *in silico* simulations with binary replicons, thus potentially taking into account the whole mutant spectrum of these quasispecies. The results of these simulations are in complete agreement with the mean field model. In general, the conclusions drawn from the CA model are in excellent agreement with the mean field analysis and with the *in silico* simulations, although the spatial structure is shown to broaden the conditions at which the survival-of-the-flattest may occur. This result is of clear relevance for the experimental data supporting the applicability of the survival-of-the-flattest hypothesis to viral populations and in particular to the observations of Codoñer et al. (2006) with viroids and by extension to plant viruses. Plant viruses replicate and systematically move within infected plants forming spatially structured patchy populations rather than a single well-mixed population (Dietrich and Maiss 2003, Hall et al. 2001, Jridi et al. 2006). Different leaves may not necessarily be infected with the same virus genotype and, even within a single infected leaf, different genotypes may not coinfect the same cell and thus, not compete each other intracellularly. This being the case, a flat quasispecies may increase its frequency in the metapopulation by avoiding direct competition with the fit quasispecies even at low mutation rate.

Antiviral drugs with mutagenic action (e.g., nucleoside analogues like ribavirin) have been widely used, in combination with other drugs or interferons, as antiviral therapies against HIV-1 and *Hepatitis C virus*. However, a classic observation is that drug-resistant virus readily emerged upon treatment (Gao et al. 1992, Keulen et al. 1999, Larder and Kemp 1989, Pfeiffer and Kirkegaard 2003). In general, these resistant mutants present mutations at the polymerase gene which enhance fidelity at the cost of lowering replication down. In addition to this mechanism of resistance, flat quasispecies might provide an alternative way of escaping from mutagenic therapies. In this sense, Sanjuán et al. (2007) have recently shown robust populations of VSV, an animal RNA virus, that were able of outcompeting the fittest wildtype in the presence of high concentrations of mutagens. These findings, along with our theoretical results, have clear implications for the evolution of drug-resistant viral strains *in vivo*. When the mutagen has a high concentration across host tissues, robust quasispecies can be selected and dominate the viral population. After suppression of the mutagenic therapy, wildtype would come back owing to its replicative advantage and, thus shall increase its frequency in the population. However, if flat quasispecies are spatially confined into reservoirs, then our results show that the time required to eliminate them from the population will be much longer than expected for the case of a well-mixed single population.

Altemeyer, S. and McCaskill, J. S. [2001]. Error Threshold for Spatially Resolved Evolution in the Quasispecies Moedel. *Phys. Rev. Lett.*, 86(25):5819–22.

Bordería, A. V., Codoñer, F. M., and Sanjuán, R. [2007]. Selection promotes organ compartmentalization in HIV-1: evidece from gag and pol genes. *Evolution*, 61:272–279.

Codoñer, F. M., Daròs, J. A., Solé, R. V., and Elena, S. F. [2006]. The fittest versus the flattest: Experimental confirmation of the quasispecies effect with subviral pathogens. *PLOS Pathog.*, 2(12):e136. doi:10.1371/journal.ppat.0020136.

Dietrich, C. and Maiss, E. [2003]. Fluorescent labeling reveals spatial separation of potyvirus populations in mixed infected "*Nicotiana benthamiana*" plants. *J. Gen. Virol.*, 84:2871–2876.

Domingo, E. [2002]. Quasispecies theory in virology. *J. Virol.*, 76:463–465.

Domingo, E. and Holland, J. J. [1997]. RNA virus mutations and fitness for survival. *Annu. Rev. Microbiol.*, 51:151–178.

Eigen, M., McCaskill, J., and Schuster, P. [1988]. Molecular Quasispecies. *J. Phys. Chem*, 92:6881–6981.

Eigen, M. and Schuster, P. [1979]. *The Hypercycle. A Principle of Natural Self-Organization*. Berlin: Springer–Verlag.

Gao, Q., Gu, Z. X., Parniak, M. A., Li, X. G., and Wainberg, M. A. [1992]. In vitro selection of variants of Human immunodeficiency virus type 1 resistant to 3'-azido-3'deoxythymidine and 2',3'-dideoxyinosine. *J. Virol.*, 66:12–9.

Hall, J. S., French, R., Hein, G. L., Morris, J., and Stenger, D. C. [2001]. Three distinct mechanisms facilitate genetic isolation of sympatric Wheat streak mosaic virus lineages. *Virology*, 282:230–236.

Holmes, E. C. and Moya, A. [2002]. Is the quasispecies concept relevant to RNA viruses ? *J. Virol.*, (76):460–465.

Jenkins, G. M., Worobey, M., Woelk, C. H., and Holmes, E. C. [2001]. Evidence for the non-quasispecies evolution of RNA viruses. *Mol. Biol. Evol.*, 18:987–994.

Jridi, C., Martin, J. F., Mareie-Jeanne, V., Labonne, G., and Blanc, S. [2006]. Distinct viral populations differentiate and evolve independently in a single perennial host plant. *J. Virol.*, 80:2349–2357.

Keulen, W., van Wijk, A., Schuurman, R., Berkhout, B., and Boucher, C. A. [1999]. Increased polymerase fidelity of lamivudine-resistant HIV-1 variants does not limit their evolutionary potential. *AIDS*, 13:1343–9.

Larder, B. A. and Kemp, S. D. [1989]. Multiple mutations in HIV-1 reverse transcriptase confer high-level resistance to zidovudine (AZT). *Science*, 246:1155–1158.

Li, H. and Roossinck, M. J. [2004]. Genetic bottlenecks reduce population variation in an experimental RNA virus population. *J. Virol.*, 78:10582–10587.

Pfeiffer, J. K. and Kirkegaard, K. P. [2003]. A single mutation in poliovirus RNA-dependent RNA polymerase confers resistance to mutagenic nucleotide analogs via increased fidelity. *Proc. Natl. Acad. Sci. USA*, 100:7289–7294.

Sacristán, S., Malpica, J. M., Fraile, A., and García-Arenal, F. [2003]. Estimation of population bottlenecks during systemic movement of Tobacco mosaic virus in tobacco plants. *J. Virol.*, 77:9906–9911.

Sanjuán, R., Codoñer, F. M., Moya, A., and Elena, S. F. [2004]. Natural selection and the organ-specific differentiation of HIV-1 V3 hypervariable region. *Evolution*, 58:1185–1194.

Sanjuán, R., Cuevas, J. M., Furió, V., Holmes, E. C., and Moya, A. [2007]. Selection for robustness in mutagenized RNA viruses. *PLoS Genet*, 3(6):e93.

Schuster, P. and Swetina, J. [1988]. Stationary mutant distributions and evolutionary optimization. *Bull. Math. Biol.*, 50:635–660.

Solé, R. V. and Bascompte, J. [2006]. *"Self-organization in complex ecosystems. Monographs in Population Biology"*. Princeton University Press, Princeton.

Solé, R. V., Ferrer, R., González-García, I., Quer, J., and Domingo, E. [1999]. Red Queen dynamics, competition and critical points in a model of RNA virus quasispecies. *J. theor. Biol.*, 240(3):353–359.

Solé, R. V., Sardanyés, J., Díez, J., and Mas, A. [2006]. Information catastrophe in RNA viruses through replication thresholds. *J. theor. Biol.*, 240(3):353–359.

Toyabe, S. and Sano, M. [2005]. Spatial supression of error catstrophe in a growing pattern. *Physica D*, 203:1–8.

van Nimwegen, E., Crutchfield, J. P., and Huynen, M. [1999]. Neutral evolution of mutational robustness. *Proc. Natl. Acad. Sci. USA*, 96:9176–9720.

Wilke, C. O. [2001a]. Adaptive evolution on neutral networks. *Bull. Math. Biol.*, 63:715–730.

Wilke, C. O. [2001b]. Selection for fitness versus selection for robustness in RNA secondary structure folding. *Evolution*, 55(12):2412–2420.

Wilke, C. O., Jia Lan Wang, Charles Ofria, Richard E. Lenski, and Cristoph Adami [2001]. Evolution of digital organisms at high mutation rates leads to survival of the flattest. *Nature*, 412(19):331–333.